Isochoric cryopreservation

Bruno Miguel Soares Guerreiro, 58721

Programa Doutoral em Bioquímica (Especialidade em Biofísica)

Para obtenção da UC: Módulo Especializado em Biofísica I

Preamble

This report constitutes the theoretical basis and analytical rationale conducted for the paper "**Enhanced Control Over Ice Nucleation Stochasticity Using a Carbohydrate Polymer Cryoprotectant**", published in *ACS Biomaterials Science & Engineering* (Vol. 8, Issue 5, 2022), in a collaboration with Prof. Boris Rubinsky, celebrated under a Fulbright Visiting Student Researcher fellowship at the University of California-Berkeley, United States of America. The emergence of isochoric systems in the field of cryobiology provides a novel pathway to study the effect of several molecules in biological systems under freezing, by allowing to probe nucleation events before the onset of crystallization. In this report, I document the theoretical basis of the technique, the design and construction of the equipment, the data analysis from a perspective of procedures employed and difficulties encountered, and future prospects of the field. Ultimately, this work emphasizes the skillset obtained in the fields of mechanical engineering, ice-based interfacial physics, and cryobiology.

Table of Contents

Introduction

1.1. Current State of Research

The World Health Organization report states that 730,000 deaths per year can be attributed to end-stage organ disease [1]. Organ and tissue transplantation are currently the only medical technique for the treatment of terminal tissue and organ failure, but it remains an intricate endeavor due to histocompatibility issues, donor-acceptor transportation logistics and timing. However, the major bottleneck leading up to this crisis is the inability to long-term preserve living tissue: the organ shelf-life times are still exceedingly inferior to the procedural time required to collect a donor organ, find a suitable acceptor, transport the organ, and transplant it. For instance, harvested hearts and lungs can barely survive for more than 6 hours, even in static cold storage [2]. With such a short biological window, 66% of hearts and 26% of livers end up losing their function. Additionally, for every patient requiring an organ transplant, the demand is 10-times higher [3]. Tissue engineering offers promising organ-on-demand solutions and highlights the possibility for establishing organ biobanks, but without an efficient method to preserve the engineered assets, funding and production are halted. It is estimated that solving biopreservation limitations could prevent more than 30% of disease-related deaths in the United States alone [1], which amounts to more than 800,000 lives. A key element in successful cryopreservation is the use of cryoprotective agents (CPAs) that aid in the survival of biological matter at low and cryogenic temperatures, such as glycerol and DMSO. However, the concentrations at which all CPAs are employed to have an appreciable effect are cytotoxic, and there are currently no means of alleviating or neutralize cytotoxicity, thus limiting their use [4]. Thus, cryoprotectant alternatives have been procured extensively, leading to research on bio-based, biodegradable polymers, which benefit from their inherent biocompatibility. Using biotechnological tools, we have previously demonstrated the ability of FucoPol, a fucose-rich biopolysaccharide produced by *Enterobacter* A47, to protect human cells against cryo-related injury [5–8]. Its strong antifreeze activity is due to a strong non-colligative influence in the freezing point of water (thermal hysteresis), which leads to ice crystals of reduced dimensions (up to 10-times smaller), thus innocuous to biologics, ensuring cell survival. Structural studies have also highlighted that FucoPol shows a strong ice-binding modulatory behavior (*under review*), similar to the Gibbs-Thomson binding mechanism of cold-adapted antifreeze proteins (AFPs). To the best of our knowledge, this was the first time a bio-based

polysaccharide was characterized to possess an AFP-like behavior. While cryoprotectants depress the freezing temperature colligatively, AFPs non-colligatively bind to particular facets of the ice crystal and promote growth on unusual facets [9]. This effect is 500 times more potent [10] than small-molecule CPAs, but AFPs are very expensive to purify and implement into cost-efficient cryoprotective formulations, thus leading to the pursue of biotechnology-based added-value alternatives.

1.2. Background in preservation methodologies

The behaviors of water and its solutions in a metastable or supercooled state have piqued the interest of researchers for decades, with applications in atmospheric and planetary sciences, agriculture, aviation, desalination, among others. Many studies have characterized aqueous supercooling (nigh-exclusively at the droplet scale) for the sake of understanding and modelling physical processes in nature. Over the last decade however, biopreservation has generated significant interest in aqueous supercooling due to its societal urgency. In a series of landmark studies [11–14], researchers have demonstrated that by maximizing supercooling, i.e. working to prevent ice nucleation and hold supercooled water in an indefinitely stable liquid state, the long-sought goal of ice-free sub-zero centigrade preservation of biological matter can be achieved, with dramatic implications in the medical preservation of human cells, tissues, and organs for transplant, preservation of sensitive foodstuffs, preservation of vaccines and other pharmaceuticals. However, while significant progress on supercooled biopreservation has been made via rigorous application of bioengineering principles to very mildly supercooled systems (held at 1–3°C below the atmospheric freezing point), further advancement in the field has largely stalled (and translation to the clinic has proven difficult) due to the stochastic nature of ice nucleation, which dictates that the probability that a supercooled system will remain stable (i.e. the probability that ice will not form) be a complex function of temperature, system size, and supercooling duration. This inherent stochasticity complicates engineering design of supercooled systems and limits the depths of temperature that can be achieved whilst maintaining reasonable confidence in the stability of the metastable supercooled state. As such, methods by which to reduce the stochasticity of ice formation, bringing it closer to deterministic behavior and thereby empowering better rational design of supercooling protocols, are urgently sought.

1.3. Isochoric *vs*. isobaric cryopreservation

Cryopreservation is based on a multidisciplinary blend of chemical and engineering solutions. During the last two decades, the group of Prof. Rubinsky developed an alternative concept to conventional (isobaric) cryopreservation, isochoric cryopreservation [15]. In isobaric (constant pressure) systems, such as a conventional freezer, all biological matter freezes and additives are sought to overcome the freezing lethality. In this setting, the system follows Gibbs thermodynamics. In isochoric (constant volume) systems, pressure is modulated in a constant-volume container, and the system behaves according to Helmholtz thermodynamics, which instead of creating a single frozen phase, allows water and ice to coexist in thermodynamic equilibrium. In this two-phase system, their proportion is mediated by fine-tuning the pressure [15]. An implication of this method is that an organ can technically be cryopreserved without ever coming into contact with the damaging ice fraction (**Figure 1**). Different chemical additives will yield unique isochoric phase diagrams due to the way they interact with water, either by contributing to freezing, supercooling or vitrification [16]. Therefore, the implementation of an isochoric methodology shifts the importance of a chemical additive from *being the essential cryoprotectant* and osmotic regulator molecule of cells, to a compound that affects the thermodynamic process of freezing in the entire system. But despite the increased benefits of isochoric preservation, a major drawback is the inability to control *when* and *where* nucleation will occur in the system. One can plant a nucleation seed in strategic spatial locations, such that crystallization in the system can occur spatially separated from the biological matter, but the moment at which this nucleation-to-growth progression occurs has remained uncontrollable. Hence, the search for cryoprotectants capable of also influencing the nucleation stage, rather than simply the crystallization stage, is of highest priority.

Isochoric preservation is a novel technique, whose thermodynamic principles had only been characterized with water, simple salt solutions (*e.g.* NaCl) and common cryoprotectants (*e.g.* glycerol, ethylene glycol) [15]. Here, we characterized for the first time the influence of the first biopolymer, FucoPol, in isochoric thermodynamics [7]. FucoPol was selected as the model molecule for this study due to (i) its previously demonstrated cryoprotective properties [6], (ii) a very low osmolality-to-function ratio that reduces mass transport and is capable of competing with

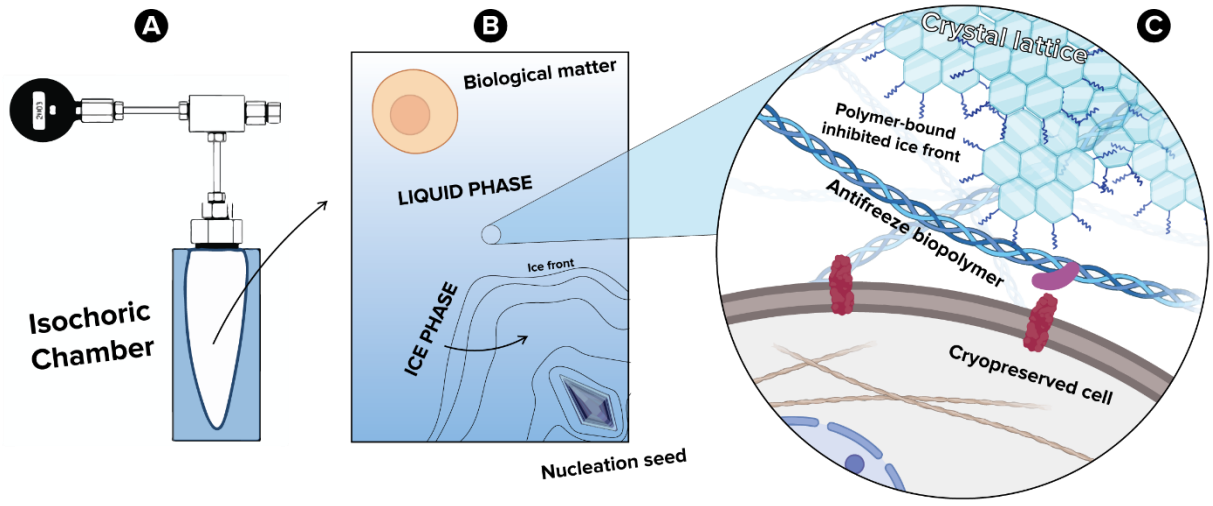

Figure 1. Representation of the isochoric cryopreservation process. A constant volume, pressurized chamber (A) is filled with fluid and cooled by immersion. Inside (B), a nucleation seed induces crystallization in a corner safely distant from biological matter. The addition of an antifreeze biopolymer (C) further protects cells from cryoinjury.

antifreeze proteins, (iii) a high viscosity associated with high molecular weight [17], and (iv) an intrinsic biocompatibility that eliminates cytotoxicity issues. Previous work under isobaric conditions has shown that FucoPol induces the occurrence of crystallization at a higher temperature, consistent with the results herein, and that there is a concomitant 54% reduction of mean crystal size and a distinguishable effect on crystal morphology [5].

1.4. Isochoric Thermodynamics

A thermodynamic process that occurs at constant volume, with varying temperature and pressure, is said to be an isochoric process. This means that any work, *dW*, done by or on the system is decoupled from a volumetric change, *dV*, and the only way for the system to exchange energy is through heat transfer, *dQ*. Mathematically, this can be conveyed as follows:

$$dU = dQ - dW = dQ - pdV \xrightarrow{dV = 0} dU = dQ \quad \text{(Eq. 1)}$$

The Gibbs free energy, ***G***, is often used in biochemical systems to express the thermodynamic potential that governs the spontaneity of occurrence of chemical reactions and can be expressed as follows:

$$G = U - TS + pV \quad \text{(Eq. 2a)}$$

$$dG = dU - TdS + pdV \quad \text{(Eq. 2b)}$$

However, ***G*** implies that biochemical processes occur at constant pressure (atmospheric). In an isochoric system, the governing thermodynamic potential is the Helmholtz free energy, ***F***:

$$F = U - TS \quad \text{(Eq. 3a)}$$

$$dF = -SdT - pdV \quad \text{(Eq. 3b)}$$

As no *pV*-work is done in an isochoric system, this relation essentially states that any change in internal energy at a given temperature arises from a change in entropy *dS*. The Helmholtz potential ***F(T,V)*** then differs from the Gibbs potential ***G(T,P)*** with regards to volume being constant, rather than internal pressure. The volumetric thermal expansion of ice β_T is a positive quantity, which means during a water-to-ice phase change, the confined volume will expand. However, due to the volume-constrained nature of non-deformable isochoric chambers, an increase in internal pressure occurs instead. Hence, the primary metric to probe in an isochoric chamber is **pressure**. Although non-deformable by principle, the isochoric chamber does undergo reversible microscopic strain stress, which can be detected by a strain gauge sensor. Thus, electrical signal transduction is the main source of isochoric nucleation detection data. At given *T*, a significant spike in internal pressure change relates to a volume-independent change in internal energy, such as the onset of a phase transition. In thermodynamics, the first event in a phase transition arising from freezing the system that relies on a molecular re-arrangement – and leads to a change in internal energy – is nucleation.

1.5. Nucleation

A body of water completely filling a non-deformable recipient constitutes a one-phase isochoric system. Upon cooling, water molecules start to arrange into unstable molecular clusters, which are of transient nature due to punctual, localized thermal fluctuations. The sum average of these fluctuations is a measure of entropic variation inside the system. If a liquid is cooled down slow enough below its freezing point, it enters a supercooled regime which, over time, increases the

probability of molecular cluster formation and growth. Once these unstable clusters grow to a critical nuclei radius r_c, they become stable, do not redissolve, and act as nucleation seeds from which system-scale crystallization can proceed. The nucleation stage is still not energetically favorable ($\Delta G > 0$), but a trade-off between volumetric and interfacial energies, ΔG_v and ΔG_s (**Figure 2**).

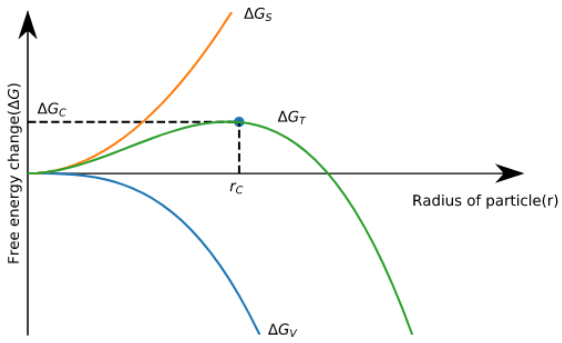

Figure 2. The energetic landscape governing nucleation (green), mediated by counteracting volumetric (blue) and interfacial (orange) energy curves. Any nuclei aggregates satisfying $r < r_c$ are unstable and redissolve. Stable nuclei for which $r > r_c$ satisfy a survivorship bias and act as nucleation seeds for crystallization to occur spontaneously ($\Delta G < 0$), continuing until thermodynamic equilibrium is achieved.

For an ice nucleus to evolve into a crystal, its growth will follow the energetic landscape presented in **Figure 2** until it reaches a radius r_c. The Gibbs free energy for nucleation, ΔG_n is a gain-cost function counteracting nuclei-water interfacial tension ($\Delta G_s > 0$) and the amount of clustered water molecules ($\Delta G_v < 0$):

$$\Delta G_n = \Delta G_v + \Delta G_s = \frac{4}{3}\pi r^3 \Delta g_v + 4\pi r^2 \gamma \qquad \text{(Eq. 4)}$$

where ΔG_v is the Gibbs free energy per unit-volume and γ is the surface tension. The point at which cluster volume overcomes energetic contributions from surface shape geometry ($r=r_c$) implies that the energy barrier for nucleation is surpassed ($dG_n=0$) and unstable clusters become stable, not re-dissolving. Classical Nucleation Theory (CNT), initially formulated by Volmer, Weber and Farkas in 1927, states that the nucleation process is stochastic, which means that the occurrence probability of nucleation can be precisely defined for a range of temperatures but cannot be

pinpointed to a single temperature [18]. Thus, the approach to modeling the nucleation of crystals in a supercooled liquid is of statistical nature. The number of critical size nuclei formed per unit time, the nucleation rate, *J*(T), may be estimated by the following power-law:

$$J(T) = J_0 \times e^{\left(-\frac{\Delta G_n}{kT}\right)} = \gamma \Delta T^n \quad \text{(Eq. 5)}$$

where J_0 is a constant, ΔG_n is the activation energy barrier for nucleation, k is the Boltzmann constant and T is the temperature, γ and n being empirical parameters. The constant cooling rate experiments presented in this study can be modelled as a non-homogeneous Poisson process [19], whereby the fraction of unfrozen samples at a given temperature, $\chi(T)$, can be related to $J(T)$ as follows:

$$\chi(T) = e^{\left(-\frac{1}{\beta}\int_{T_m}^{T} J(T)\, dT\right)} = e^{\left(-\frac{\gamma}{\beta}\cdot\frac{(T-Tm)^{1+n}}{1+n}\right)} \quad \text{(Eq. 6)}$$

where T is the temperature, T_m is the equilibrium melting point, β is the cooling rate, and γ and n are empirical fitting parameters. Here, T_m = 0ºC due to a proven non-colligative effect of FucoPol on water thermodynamics [5], and β = 2ºC/min. Lastly, the behavior of a thermodynamic system at a given temperature and solute concentration can be better grasped by plotting induction time graphs (see **Figure 9b**). The mean induction time, τ, describes how long a system will remain in stable supercooled state before the first super-critical ice nucleus emerges. It is inversely proportional to the nucleation rate, $J(T)$, as follows:

$$\tau = J(T)^{-1} \quad \text{(Eq. 7)}$$

1.6. Objective

The aim of this project was to pursue a fundamental thermodynamic characterization of a biopolymeric isochoric system. FucoPol is an interesting compound because of its AFP-like activity, crystal size reduction and cytotoxicity-free alternative, but also represents a formidable challenge in biophysics due to its complex structure. We believe that exploring the isochoric cryopreservation boundaries with FucoPol as a model antifreeze biopolymer is a fundamental step

into unveiling new biopreservation solutions. This cutting-edge study created exciting opportunities for understanding deeper structure-function relationships between bio-based polymer structures and ice avoidance.

Experimental workflow

The laboratory of Rubinsky has developed unique experimental tools to study the thermodynamic properties of isochoric systems at sub-freezing temperatures and experimental tools to study the process of ice crystal growth at the microscale. The isochoric chamber uniquely available in the Rubinsky laboratory can provide real-time monitoring of the pressure and temperature inside the chamber, which can withstand pressures of up to 300 *MPa* and allows to draw fundamental concentration-dependent pressure–temperature phase diagrams for solutions of FucoPol. To the best of our knowledge, such phase diagrams have not been developed for any biopolymer.

2.1. The isochoric chamber

In an isochoric system, Helmholtz thermodynamics state that a temperature change will be coupled to an entropic effect. If volume is constant, pressure alone allows to probe the evolution of a system where two phases coexist. Isochoric nucleation of supercooled water is an example of an ice-free system, i.e. supercooled, that will eventually evolve into a two-phase phase at equilibrium. During the supercooling window, one can probe the temperature at which a rearrangement of water molecules finally occurs without generating a phase-change, i.e. isochoric nucleation, by probing a pressure spike. **Figure 3** shows several isochoric chambers, which are the core component of the isochoric system. This is where solutions are probed for their influence in the nucleation temperature, and the most critical quality control step was to ensure that nucleation would only occur as an influence of the test molecule, and not related to chamber design.

2.1.1. Design tenets

First, a 7075 aluminium alloy chamber is cleaned and polished before first use, and a strain gauge (the pressure sensor) is superglued to a flat wall of the container. Although initial designs for the isochoric chamber were rectangular (Figure 3*a*), a cylindrical shape was preferred for external aesthetics and weight reduction, but the critical reason was to remove small angle corners inside the chamber, which would promote nucleation. However, applying a strain gauge to curved

cylindrical walls would result in artefactual measurements of strain due to the curvature of the sensor. Thus, a trade-off hexagonal shape of external flat walls (unto which the strain gauge was applied) and internal cylindrical hollowing (which minimized heterogenous wall-based nucleation) was considered optimal (Figure 3*c*). In the case of an isochoric chamber designed for vitrification (Figure 3*b*), the cold immersion (to –196ºC in liquid nitrogen) destroyed the strain gauge microchip, thus opting for an external strain gauge cable that would be placed on top of the container cap instead (*not shown*). Therefore, the cylindrical design could be maintained.

Figure 3. An assortment of isochoric chamber designs. (a) The first prototypes of aluminium alloy-based isochoric chambers, from small to large-scale containers. (b) The final design of a 5-ml isochoric chamber optimized for vitrification experiments. The blue color represents an anodized alloy which coats the titanium to increase durability and resistance to corrosion. (c) The initial chamber preparation involves supergluing a strain gauge (brown) element to the chamber, which provides accurate pressure changes inside the chamber that reflect nucleation events taking place. The small, bored hole above the strain gauge ("gaping hole"), is strategically placed to allow liquid overflow, and indicates when the chamber is completely filled with solution.

2.1.2. Preparation

The most critical step in ensuring a functional isochoric chamber is the proper attachment of the strain gauge. An accurate determination of internal pressure is required for isochoric nucleation event detection and is therefore the essential probing element. **Figure 4** summarizes the preparation steps employed when preparing a novel isochoric chamber for isochoric nucleation measurements for the first time. After this stage, the chamber is always ready-to-use for further experiments. First, the chamber surface was cleaned with ethanol or acetone (*1*). The wet surface was sanded with sandpaper (150–400 grit) to roughen the surface, in alternate directions to avoid etching grooves (*2*). After sanding, the surface was continuously cleaned with the previous solvent

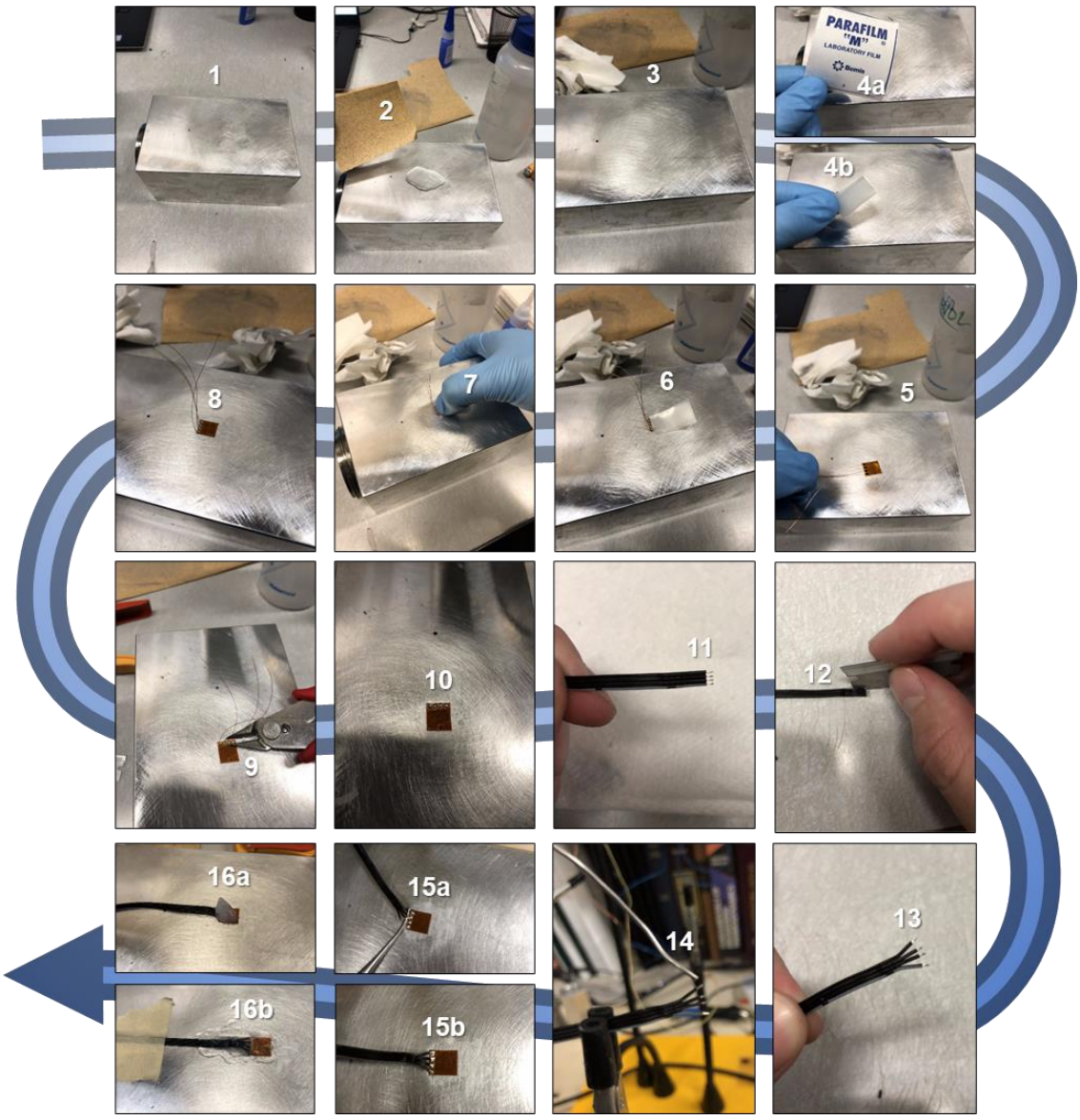

Figure 4 – Preparation of the isochoric chamber, with strain gauge attachment.

to remove any debris until none remained (*3*). Then, a single square of parafilm (*4a*) was cut and folded into a tab (*4b*), to be used to press and hold the strain gauge in place while the glue set. A single drop of superglue was applied to the bottom side of the strain gauge (*5*), whose face is flat and does not contain soldering terminals. The strain gauge was placed onto the chamber surface with the lead wiring point towards the top of the chamber ("gaping hole" direction) and bent upwards so as to not become glued to the surface (*6*). This step was critical as the wiring would be trimmed off later. Then, the strain gauge is cautiously pressed against the wall for a few moments to allow the glue to set (*7*) and left to dry for 10–15 minutes (*8*). Then, the preinstalled wires to the

base of terminals were trimmed (*9*) and it was ensured that any exposed remaining wire was not in electrical contact with the chamber (*10*). Then, a length of ribbon cable was cut and stripped back to less than 5 mm of insulation (*11*). A razor blade was used to separate individual wires (*12*), taking caution to not pierce insulation (*13*). The wire tips were pre-applied with solder (*14*) and soldered one at a time to the strain gauge terminals (*15a*), ensuring that each was electrically isolated from one another and from the chamber. The final result is seen in *15b*. Lastly, a dollop of epoxy (Sil-Poxy™) was applied as protective coating to the strain gauge (*16a*). The epoxy was carefully spread on top and underneath wires to ensure a thin, non-bulging coating, yet thick enough to protect wiring and strain gauge. The final product was let dry for 24 hours and is observed in *16b*.

2.1.3. Coating

After the isochoric chamber is prepared for the intended use (whether it is a supercooling or vitrification experiment), the internal walls of the chamber are first coated with pre-heated petrolatum (Vaseline, Unilever, UK) to further minimize heterogenous nucleation in the internal walls of the chamber (**Figure 5**). Any concave irregularities in the wall would provide a nucleation site to water molecules, thus introducing experimental bias in the result, to which it was found that a uniform hydrophobic coating minimized this effect. So far, the most cost-effective substance for such an application has been found to be common-grade commercial Vaseline. Procedural-wise, 1 mL of vaseline is first applied in its solid form with a stainless-steel lab spatula, in a good amount. Then, a handheld torch is used to heat the Vaseline for about 5 minutes, to decrease its viscosity and allow it to flow. After visible melting of the petrolatum, the isochoric chamber was inverted, rotated to allow for uniform coating of the walls and remove excess fluid, and placed at –4ºC upside down until the Vaseline solidified. By gravimetric principles, the same coating thickness is consistently obtained because the adhesive-cohesive properties of vaseline are a fixed molecular property, such that in case of excess vaseline, a fixed amount will coat the walls, the only change being in the excess amount that overflows.

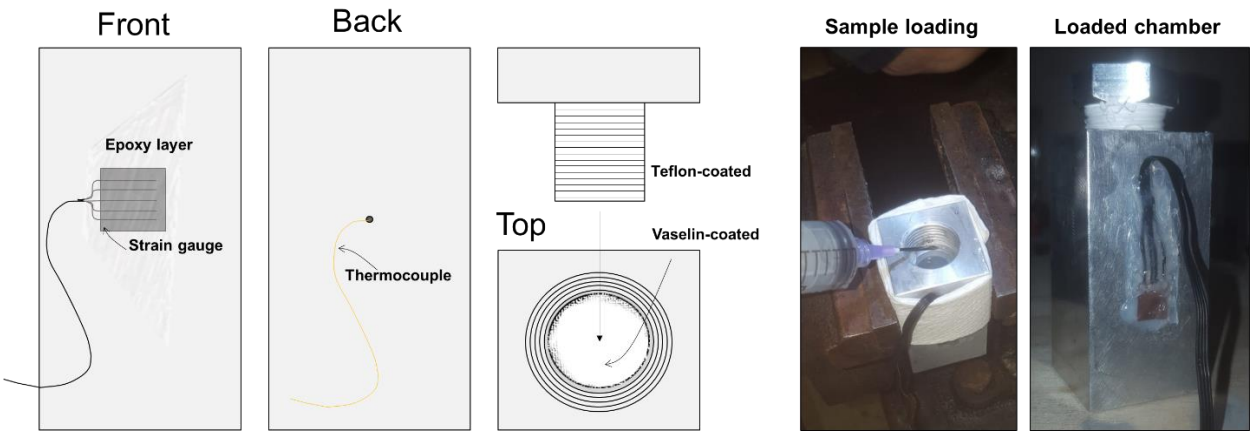

Figure 5 – Schematics of a functional isochoric chamber, and internal coating procedure.

2.1.4. Loading

Upon solidification of the inner coating, a 5.4-ml liquid solution was slowly applied to the isochoric chamber by careful diagonal dispensing of a syringe to avoid any bubbling. The solution applied must be degassed in a vacuum chamber for at least 30 minutes prior to use to remove bubbles which act as heterogenous ice nucleators, and very cautiously syringed diagonally into the walls of the isochoric chamber, to avoid any bubbling **(Figure 5)**. In polymeric solutions, this step is critical due to the high viscosity which prevents gas phase diffusion and the cavitation induced from mixing. With the isochoric chamber properly loaded, the chamber plug (cap) is coated with Teflon in the direction opposite to the rotation of the closing motion of the chamber, to ensure proper seal, and its bottom surface also thinly coated with petrolatum. Any overflow is removed through the *gaping hole* after closure. Then, the chamber was placed in a bench vise and the plug threads were tightened with a Yellow Jacket 60648 torque wrench by applying a sealing torque of 40 ft-lbs. The excess liquid was cleaned from the overflowing gaping hole, and the chamber is ready for experimentation.

2.2. Isochoric Nucleation Detection (INDe) apparatus

The isochoric chamber creates the boundary condition to the thermodynamic system being probed and is the thermodynamic centerpiece. However, the temperature control and real-time monitoring of pressure occurs in an external device called the isochoric nucleation detection (INDe) apparatus, which is composed of several modules:

i. **Temperature input/output:** Peltier modules and heat sink.
ii. **Temperature control and probing:** strain gauge probe, thermocouple & assemblies.
iii. **Data collection & monitoring:** Python-based control software.

An INDe is versatile because it can process a single chamber system or parallel-process multiple units, yielding a high-throughput collection of data. Figures 6–7 show the original (UC-Berkeley) and newly-built (NOVA-SST) INDe apparatuses, respectively, and further schematics of their back-end architecture.

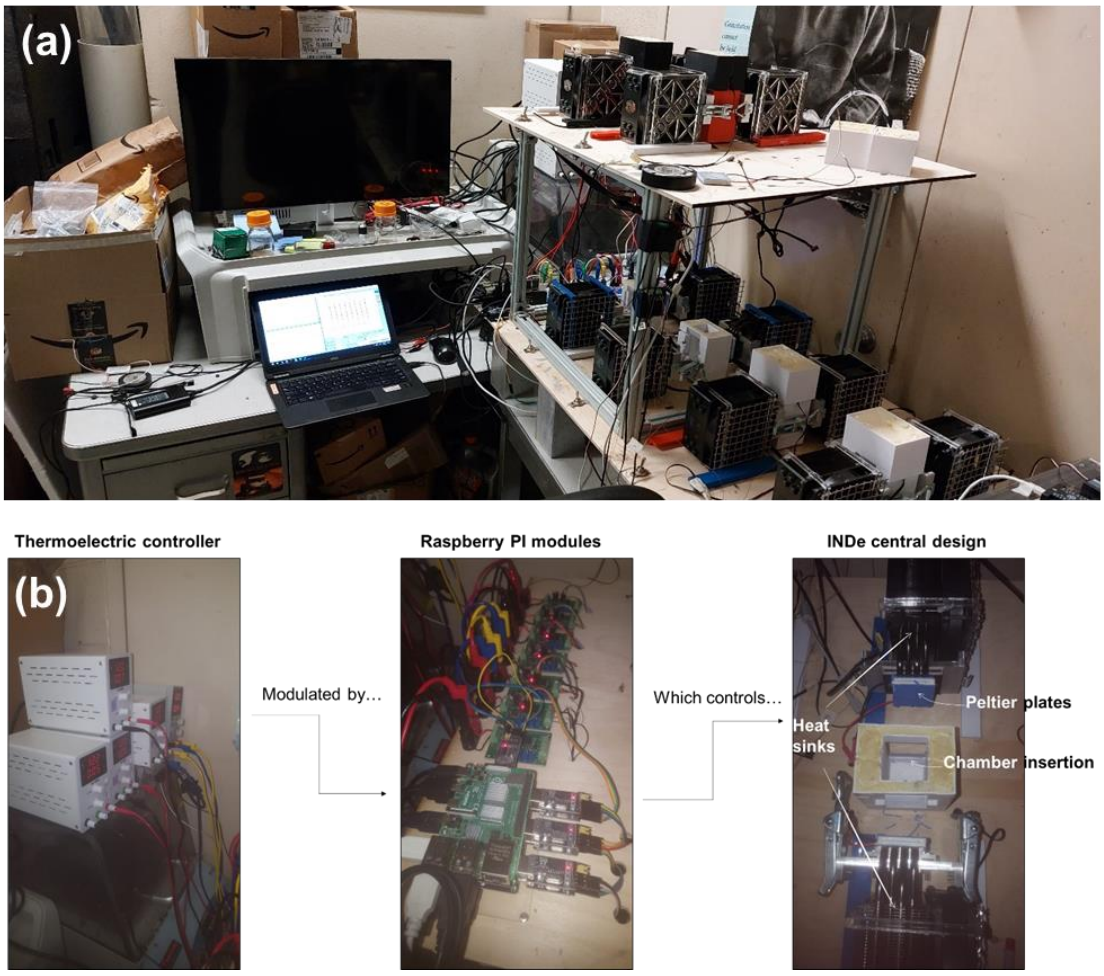

Figure 6 – The original INDe apparatus, designed by Tony Consiglio at the University of California-Berkeley, USA. Panel (a) shows a parallel assembly of several isochoric nucleation units. The ability to parallel process different freeze-thaw cycling experiments yields a high-throughput analysis. Panel (b) represents a back-end schematics of how each module is cross-connected, representing a hierarchical process tree.

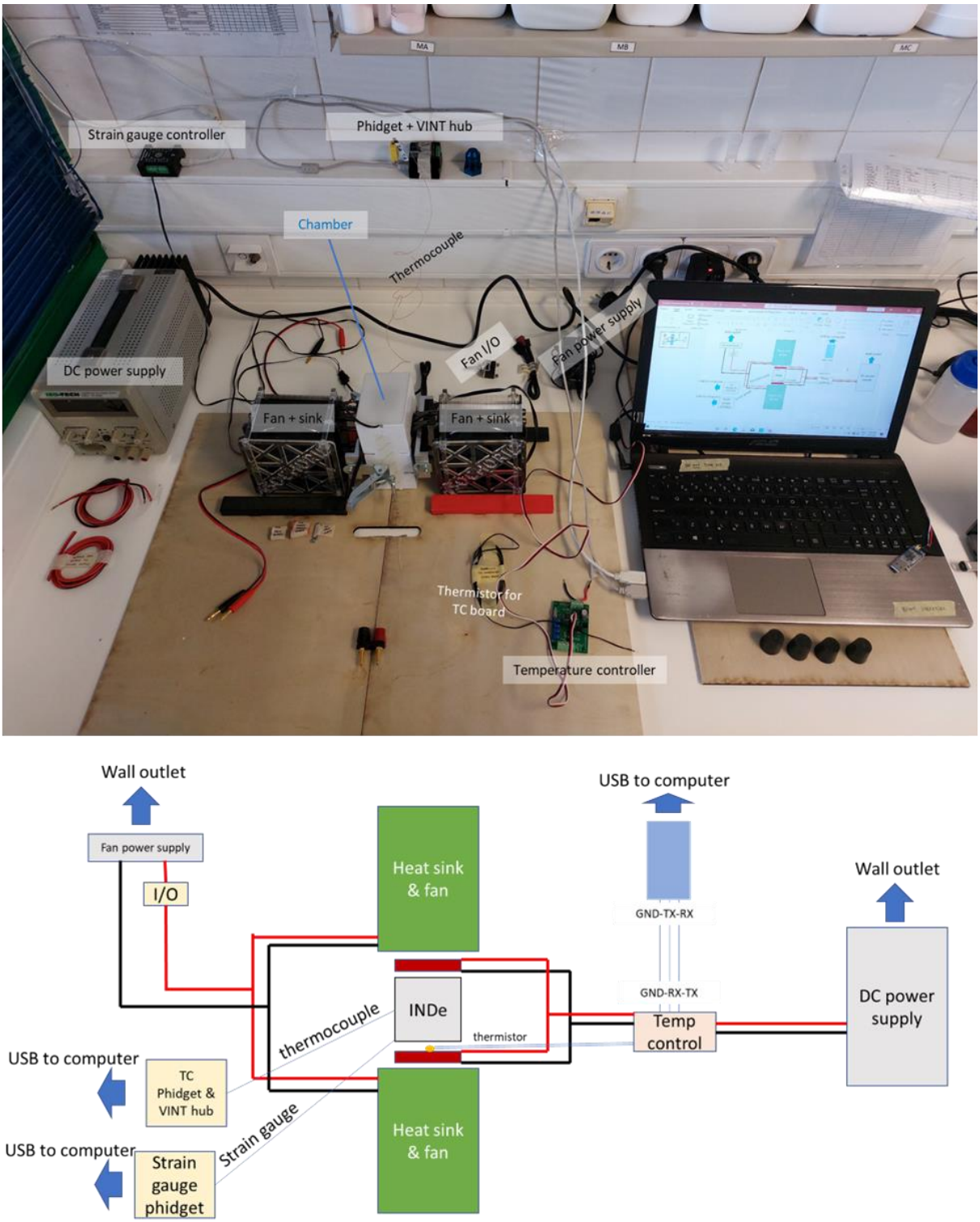

Figure 7 – The current INDe apparatus, re-built by Bruno Guerreiro at the School of Science and Technology, Nova University of Lisbon, Portugal. The top panel shows a single-unit INDe containing an isochoric chamber running an experiment. The bottom panel is a blueprint of the electrical wiring involved in the setup shown, with the isochoric chamber at the center ("INDe"), between both Peltier plates in red.

2.2.1. Setup and electronics

The INDe system, as designed by Consiglio *et al.* [20], is composed of three main components. The first component is a Python-based control software that runs on a Raspberry Pi 4B single board computer (Raspberry Pi Foundation, UK). The newly built INDe system in Portugal was adapted to run on Windows 10. The next component consists of two temperature control assemblies, each comprised of a two-stage thermoelectric module, known as multi-stage Peltier modules (CUI Devices CP60H-2 Series) and a fan-cooled CPU heat sink (Cooler Master). The last component is a thermoelectric module controlled by a PID temperature controller (Opt Lasers, TEC-8A-24V-PID-HC-RS232), which is composed of a full bridge aluminum strain gauge (3147_0), a PhidgetBridge strain gauge DAQ (1046_0B), a thermocouple Phidget DAQ (TMP1101_0) and a USB VINT Hub (HUB0000_0), all purchased from Phidgets Inc. (CA).

2.2.2. Experimental run

A solution-loaded and sealed isochoric chamber was first placed between the two Peltier modules, in the 3D-printed Styrofoam holder intentionally designed for holding the chamber. Initially, the chamber is equilibrated at 5ºC for 5 minutes. Then, a complete freeze-thaw cycle is completed, comprised of the following: cooling at –2 ºC/min until nucleation is detected by an increase in strain gauge pressure, then fast warming to 5ºC and hold for 5 minutes to guarantee full melting of the system. This cycle is repeated at least 50 times, for three different chamber preparations of the same solutions (triplicates), until about N=150 readings are obtained. The corresponding nucleation temperatures detected are recorded as a time-series, as a function of cycle number. The high number of cycles collected is related to nucleation being a stochastic event, in which a nucleation temperature is statistically associated to be recorded at a given temperature interval, but its accurate temperature datapoint cannot be known for a given cycle. Thus, a high number of cycles ensures statistical significance.

2.2.3. INDe architecture rationale

Using the helpful illustrations in Figure 7, we shall now describe the INDe experimental pathway in a sequential manner, representing how the front-end and back-end architectures cooperate:

1. With an isochoric chamber in the chamber holder, properly insulated from top and side with the Styrofoam, and in contact with both Peltier plates, the computer and all power supplies (DC and heat sink fans) are turned on.

2. The DC power supply provides energy to the ***temperature controller (TC) board***, which is connected to both the computer and both Peltier plates through electrical wiring. A thermistor is also placed inside the blue paste insulation of a Peltier module. It is through the TC board that any temperature inputs by the user are convened to control the working temperature, such as the initial holding temperature, and the automatic temperature control of the chamber through the freeze-thaw cycles.

3. On the parameter sensing architecture, two variables exist: temperature and strain. The temperature is measured by a ***thermocouple*** introduced in a external wall hole bored into the chamber (not the 'gaping hole', see **Figure 5**) and signal transduced by a TC Phidget-VINT hub couplet USB-connected to the computer. The strain is measured by the ***strain gauge***, connected to a strain gauge phidget USB-connected to the computer.

4. To enable proper temperature control, the Peltier modules are physically close to two commercial-grade computer fans, which re-circulate the air near the isochoric chamber to the external environment. This allows for accurate nucleation temperature sensing and cooling of the electrical components. By the same note, the whole INDe system should be operated in a controlled-temperature room.

2.3. Referential high-throughput nucleation profiles

The real-time monitoring of temperature and strain is shown with Python-based visualization libraries (matplotlib in this case) in the computer screen, plotting strain as a function of time. The nucleation temperatures are then collected from a signal detection algorithm specifically developed by Bruno Guerreiro for this application. This equipment can also run partially unsupervised, as it can be coupled to remote control software such as RealVNC that can start, stop, analyse and parallel-process the data from a distance, allowing real-time data collection to be performed overnight. Further safety algorithms can be flexibly implemented in the case of errors or electrical overheating, as part of a future fully unsupervised INDe development roadmap.

Figure 8 shows a collection of real-time INDe timeseries that represent stereotypical behaviors encountered during the optimization of the system. When not working properly, these issues

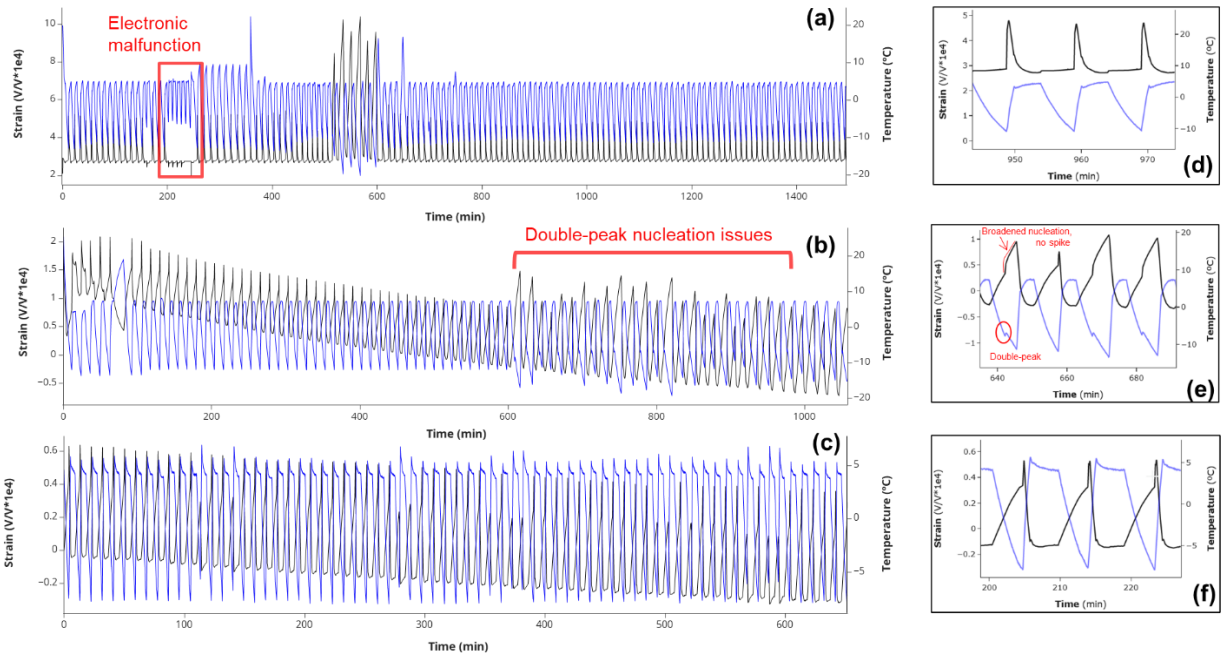

Figure 8 – First front-end real-time data collection of INDe data, which strain shown in black and temperature shown in blue. Panels *a–c* represents three stereotypical timeseries collected during the development and optimization of the INDe system, with panels *d–f* representing a zoomed-in window of the issue presented, respectively.

usually constituted one of two categories: electronic transduction or code-based sensing algorithm bugs. The normal behavior of an isochoric system is shown in **Figures 8*a/d*** (from *t*=800 min onwards) characterized by synchronous peak detection and re-equilibration of internal chamber and temperature. The thermocouple in contact with the isochoric chamber detects the internal solution temperature at a given timepoint, which is being enforced by the Peltier modules (blue lines). Concomitantly, the strain gauge detects and transduces the internal pressure the liquid is exerting in the internal chamber walls (black lines). At *t*=0 min, the hold temperature of 5ºC is detected by the thermocouple. According to the Python script, a –2ºC/min cooling rate will begin and continue until a significant 5σ spike value is detected (five standard deviations above strain baseline), at which point cooling stops and the chamber is heated back up to 5ºC for liquid-state equilibration. The time-temperature point at which a strain spike was detected corresponds to an increase in internal pressure associated with a nucleation event, and a nucleation temperature T_n is recorded for cycle *n*, which can then be data-scraped into an exportable list.

It is worth discussing common experimental issues when running the INDe, to properly troubleshoot issues in the architecture and validity of collected data:

a) One run presented an electronic malfunction (**Figure 8*a***, *t*=200–300 min) in which the absence of a strain spike was still followed by a properly working F-T cycle. In this case, abnormal signal transduction from the strain gauge phidget was found to be the issue: the strain gauge would report no increased internal pressure, but the controlling phidget resetted the temperature control cycles, leading to a non-overlap of temperature and strain lines. A simple loosening of port connectivity was the issue.

b) An improper adjustment of the strain gauge resulted in a double-peak nucleation issues, in which nucleation would be detected twice in the cooling stage (**Figures 8*b*/*e***). This was visible by a slow increase in internal pressure rather than a spike event (black) which would hint at cooling to stop and heating to resume, followed by a sharp peak which would indicate another nucleation event, thus doubling the cooling phases.

c) Lastly, bugs in the code can also lead to poor readings, in which the data collection appears valid, variable sensing appears synchronous, but signal looks abnormal (**Figures 8*c/f***). In this case, strain detection presented a slow increase in internal pressure followed by a small spike, quite similar to issue (b), but without double-peak issues. However, the onset of nucleation detection is characterized by a sharp spike from baseline, and not a cumulative increase of internal pressure, thus presenting invalid results. This problem is also possibly attributed to the presence of air bubbles in the solution, which reflect a different behavior of the liquid and skew nucleation temperature data.

Results

The isochoric nucleation data obtained for FucoPol solutions is extensively described in the paper "Enhanced Control Over Ice Nucleation Stochasticity Using a Carbohydrate Polymer Cryoprotectant", published in *ACS Biomaterials Science & Engineering* (Vol. 8, Issue 5, 2022) [7]. A wrap-up summary is hereby provided for context, and its implications briefly noted.

3.1. Theoretical basis

We performed a study probing the effect of a high molecular weight, bio-based carbohydrate polymer (FucoPol) on aqueous supercooling. We deployed a recently developed low-latency isochoric nucleation detection technique (INDe) [20] to conduct hundreds of nucleation trials on solutions of water and concentrations (up to 0.5 wt.%) of FucoPol (**Figure 9*a***), yielding a statistically powerful spread of nucleation temperatures for each concentration (**Figure 9*c***). The spread of nucleation temperatures, where each datapoint reflects the time elapsed until nucleation was detected, can be statistically interpreted as a non-homogeneous Poisson-modelled nucleation event (Eq. 6), and a mean induction time τ (Eq. 7) determined for a particular molecular system (**Figure 9*b***). From these relationships, one can fully design temperature-concentration stability maps for various cryoprotectants (**Figure 10**), from which actionable insights on system parameterization can be derived, which has implications in biological shelf-life and operational control.

3.2. Previous INDe findings: water and small-molecule behavior

The first isochoric supercooling studies by Consiglio *et al.* [20] have shown that aqueous solutions of glycerol, ethylene glycol, DMSO, and propylene glycol resulted in average nucleation temperatures of −20, −20, −21, and −22 °C, respectively, at 5 mol% (equivalent to 15.4−21.2 wt.%). Compared to pure water, these values effectively constituted a supercooling effect, inducing freezing point depression of water. Previous literature on the subject ubiquitously confirmed that most small-molecule cryoprotectants and antifreeze proteins display freezing point depression [21], thus validating the results herein. Consiglio *et al.* [20] also observed these small-molecule cryoprotectants increased the induction time τ until nucleation occurs, but did not alter the spread of nucleation temperatures nor the slope of the induction time profile.

3.3. Current INDe findings: FucoPol as model polymer

The presence of FucoPol at any concentration tested resulted in constrasting manifestations of its influence in nucleation, when compared to small molecules (**Figure 9**). While the mean nucleation temperature is minimally affected by FucoPol, rising marginally over increased concentrations as compared to pure water, the spread of the nucleation temperatures (the key manifestation of stochasticity in ice nucleation) narrows dramatically with biopolymer addition, dropping by a factor of 3 at 0.5 wt.% FucoPol (**Figure 9*a***).

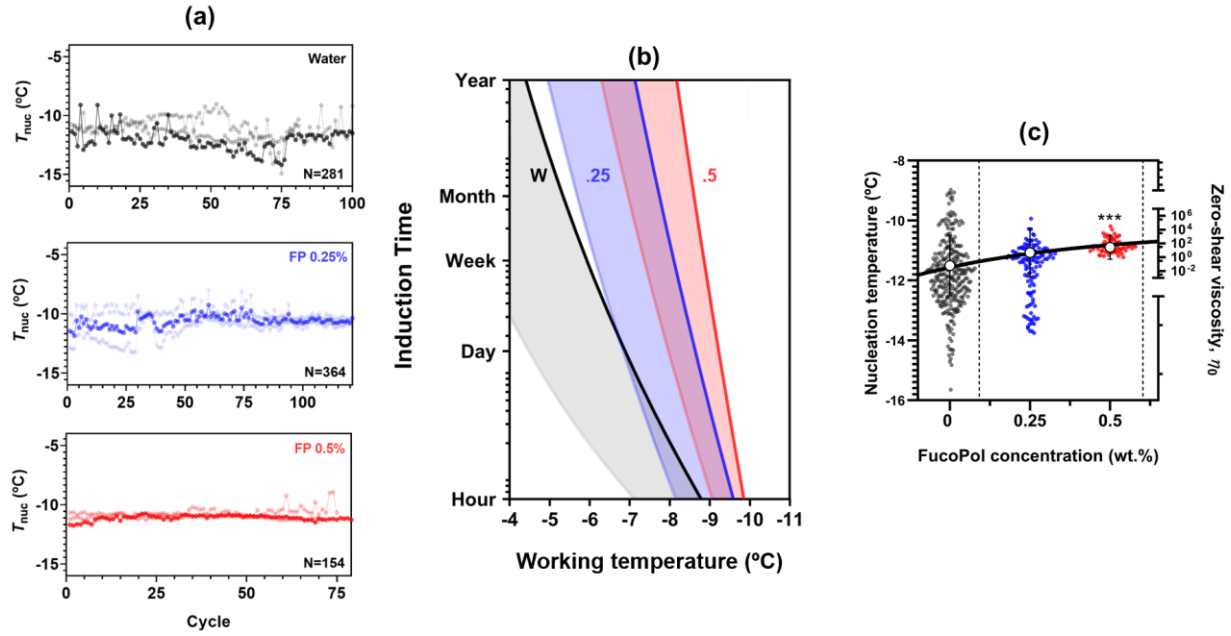

Figure 9. Summary of the influence of FucoPol on water nucleation temperature and stochasticity. (a) Nucleation cycle stochasticity runs for water (black), 0.25% (blue) and 0.5% FucoPol (red). The spread of temperature data for water is minimized with increasing polymer concentration. **(b)** Poisson-modelled induction time bands that represent the probable time elapsed until the first ice nuclei is expected to form, which provides actionable insight on on-going supercooled systems from a realistic timescale perspective. **(c)** Correlation between polymer zero-shear viscosity (black Gompertzian curve), resulting average nucleation temperature (white circle), and stochastic range (swarm plot).

This has several key implications. Firstly, it suggests that FucoPol systems are observed to follow an increasingly deterministic pattern of nucleation with respect to increased concentration (**Figure 9*c***), i.e. the stochastic temperature range is considerably reduced in its presence. Secondly, we showed using a Gompertz exponential growth model that the observed mean nucleation temperatures correlates well with the solution's zero-shear viscosity (**Figure 9*c***). Finally, by

applying a popular Poisson statistical nucleation model to the data, we demonstrated that the reduced stochasticity observed results in significantly steepened induction time curves (**Figure 9*b***), distinct from a steady-slope shift shown by DMSO and other polyols [20]. This means that small molecules linearly increased the nucleation induction time, but FucoPol generated an exponential increase, enabling longer periods of stability at temperatures above the maximal nucleation temperature as compared to pure water for equal molar increments. This also appears strongly correlated with polymeric entanglement hampering the diffusion kinetics necessary for the progressive evolution of nucleation to ice growth [17].

3.4. Actionable insights for the cryobiologist

A deeper analysis of **Figure 9*b*** allows the cryobiologist to perform statistically-driven decisions when designing a biopreservation scenario under defined conditions of temperature, solute concentration and duration of preservation. For instance, pure water in an isochoric system is expected to remain in a metastable supercooled state for about 6 months at –5ºC until nucleation initiates, but only 5 hours at –8ºC. The addition of 0.25 wt.% FucoPol at –8ºC increases system stability to two weeks, or more than a year with 0.5 wt.% FucoPol. This rationale may be conveyed more intuitively into contour plots coined as *nucleation stability maps* (**Figure 10**).

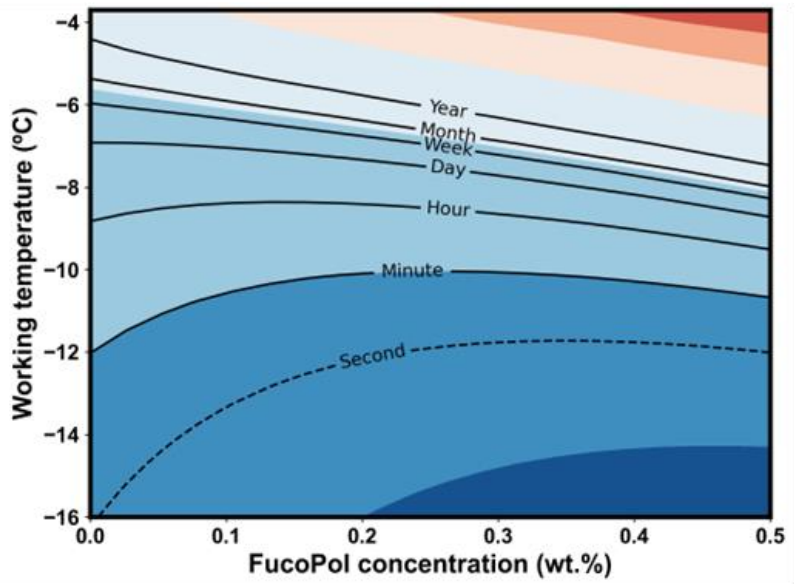

Figure 10. Final nucleation stability map for isochorically preserved systems with FucoPol. The 2D contour plot represents the information contained in induction time plots as a function of temperature but extended to molar increments in the molecular cryoprotectant used.

This substantially unique behavior of FucoPol may be employed to enhance supercooling stability at non-toxic osmolalities, leading to more efficient design of supercooled biopreservation protocols and elimination of critically damaging *rogue* nucleation events, i.e. for a particular freeze-thaw protocol, nucleation may initiate in an extreme datapoint of its characteristic temperature interval (outside the 10-90% interval range, hence *rogue*-like, or improbable but possible). While the precise mechanism of action that drives the reduction in stochasticity is just now being elucidated, it appears purely kinetic in nature (i.e. distinct from any colligative thermodynamic effects such as those for small molecules), and may be common to other high molecular weight polymers, suggesting an intriguing line of future research.

Conclusions

For the first time, a fundamental study on understanding isochoric thermodynamics with polymeric substances was performed. FucoPol, a bio-based, fucose-rich polysaccharide, was shown to be a modulatory molecular additive with very low osmolality that regulates stochasticity by confining ice nucleation to a more deterministic range of temperatures and significantly delaying the onset of nucleation. We have achieved a supercooled state of water that is 1.7−3 times more stable in the presence of FucoPol, and with drastically increased nucleation induction times that range from *ca.* 2 weeks to over a year at −8 °C, compared to only 1 h for pure water (a 2−3-fold order of magnitude increase in temporal stability). For the cryobiologist, FucoPol may present a potent tool with which to manipulate the kinetics of ice formation during supercooled biopreservation to increase the stability of supercooling and predictability of ice nucleation behavior. In practice, this increased nucleation determinism provides a procedural safety net to biopreservation strategies that rely on the isothermal hold of biological matter in a supercooled state, while also enabling higher statistical confidence during protocol design.

The research documentation presented herein,
which constituted the previously aforementioned paper,
was awarded with the ***John K. Critser Travel Award*** *for best extended abstract,*
the ***Society for Cryobiology Student Travel Award****, and nominated for*
the ***Crystal Award*** *as one of the top 5 best oral presentations,*
at the 59th Annual Meeting of The Society for Cryobiology, Dublin, Ireland (2022).

References

[1] S. Giwa, J.K. Lewis, L. Alvarez, R. Langer, A.E. Roth, G.M. Church, J.F. Markmann, D.H. Sachs, A. Chandraker, J.A. Wertheim, M. Rothblatt, E.S. Boyden, E. Eidbo, W.P.A. Lee, B. Pomahac, G. Brandacher, D.M. Weinstock, G. Elliott, D. Nelson, J.P. Acker, K. Uygun, B. Schmalz, B.P. Weegman, A. Tocchio, G.M. Fahy, K.B. Storey, B. Rubinsky, J. Bischof, J.A.W. Elliott, T.K. Woodruff, G.J. Morris, U. Demirci, K.G.M. Brockbank, E.J. Woods, R.N. Ben, J.G. Baust, D. Gao, B. Fuller, Y. Rabin, D.C. Kravitz, M.J. Taylor, M. Toner, The promise of organ and tissue preservation to transform medicine, *Nat. Biotechnol.* **35** (2017) 530–542.

[2] Buying time for transplants, *Nat. Biotechnol.* **35** (2017) 801.

[3] B. Jones, Keeping kidneys., *Bull. World Health Organ.* **90** (2012) 718–719.

[4] G.M. Fahy, Cryoprotectant toxicity neutralization, *Cryobiology* **60** (2010) S45–S53.

[5] B.M. Guerreiro, F. Freitas, J.C. Lima, J.C. Silva, M. Dionísio, M.A.M. Reis, Demonstration of the cryoprotective properties of the fucose-containing polysaccharide FucoPol, *Carbohydr. Polym.* **245** (2020) e116500.

[6] B.M. Guerreiro, J.C. Silva, C.A.V. Torres, V.D. Alves, J.C. Lima, M.A.M. Reis, F. Freitas, Development of a Cryoprotective Formula Based on the Fucose-Containing Polysaccharide FucoPol, *ACS Appl. Bio Mater.* **4** (2021) 4800–4808.

[7] B.M. Guerreiro, A.N. Consiglio, B. Rubinsky, M.J. Powell-Palm, F. Freitas, Enhanced Control over Ice Nucleation Stochasticity Using a Carbohydrate Polymer Cryoprotectant, *ACS Biomater. Sci. Eng.* **8** (2022) 1852-1859.

[8] B.M. Guerreiro, J.C. Silva, J.C. Lima, M.A.M. Reis, F. Freitas, Antioxidant potential of the bio-based fucose-rich polysaccharide fucopol supports its use in oxidative stress-inducing systems, *Polymers (Basel)* **13** (2021) 3020.

[9] H. Ishiguro, B. Rubinsky, Mechanical interactions between ice crystals and red blood cells during directional solidification, *Cryobiology* **31** (1994) 483–500.

[10] Y. Yeh, R.E. Feeney, Antifreeze Proteins: Structures and Mechanisms of Function, *Chem. Rev.* **96** (1996) 601–618.

[11] T.A. Berendsen, B.G. Bruinsma, C.F. Puts, N. Saeidi, O.B. Usta, B.E. Uygun, M.L. Izamis, M. Toner, M.L. Yarmush, K. Uygun, Supercooling enables long-term transplantation survival following 4 days of liver preservation, *Nat. Med.* **20** (2014) 790–793.

[12] H. Huang, M.L. Yarmush, O.B. Usta, Long-term deep-supercooling of large-volume water and red cell suspensions via surface sealing with immiscible liquids, *Nat. Commun.* **9** (2018) 1–10.

[13] R.J. de Vries, S.N. Tessier, P.D. Banik, S. Nagpal, S.E.J. Cronin, S. Ozer, E.O.A. Hafiz, T.M. van Gulik, M.L. Yarmush, J.F. Markmann, M. Toner, H. Yeh, K. Uygun, Supercooling extends preservation time of human livers, *Nat. Biotechnol.* **37** (2019) 1131–1136.

[14] M.J. Powell-Palm, E.M. Henley, A.N. Consiglio, C. Lager, B. Chang, R. Perry, K. Fitzgerald, J. Daly, B. Rubinsky, M. Hagedorn, Cryopreservation and revival of Hawaiian stony corals using isochoric vitrification, *Nat. Commun.* **14** (2023) 1–11.

[15] B. Rubinsky, P.A. Perez, M.E. Carlson, The thermodynamic principles of isochoric cryopreservation, *Cryobiology* **50** (2005) 121–138.

[16] Y. Zhang, G. Ukpai, A. Grigoropoulos, M.J. Powell-Palm, B.P. Weegman, M.J. Taylor, B. Rubinsky, Isochoric vitrification: An experimental study to establish proof of concept, *Cryobiology* **83** (2018) 48–55.

[17] C.A. V Torres, A.R. V Ferreira, F. Freitas, M.A.M. Reis, I. Coelhoso, I. Sousa, V.D. Alves, Rheological studies of the fucose-rich exopolysaccharide FucoPol, *Int. J. Biol. Macromol.* **79** (2015) 611–7.

[18] E. Clouet, Modeling of Nucleation Processes, *Fundam. Model. Met. Process.* **22** (2010) 203–219.

[19] D. Lilley, J. Lau, C. Dames, S. Kaur, R. Prasher, Impact of size and thermal gradient on supercooling of phase change materials for thermal energy storage, *Appl. Energy.* **290** (2021) e116635.

[20] A.N. Consiglio, D. Lilley, R. Prasher, B. Rubinsky, M.J. Powell-Palm, Methods to stabilize aqueous supercooling identified by use of an isochoric nucleation detection (INDe) device, *Cryobiology* **106** (2022) 91–101.

[21] T. Chang, G. Zhao, Ice Inhibition for Cryopreservation: Materials, Strategies, and Challenges, *Adv. Sci.* **8** (2021) e2002425.